ACS APPLIED MATERIALS & INTERFACES

Research Article

www.acsami.org

Porous Conjugated Polymer Nanotip Arrays for Highly Stable Field Emitter

Liang Zhang,[†,‡] Ke Wang,[†] Xuemin Qian,[†] Huibiao Liu,*[,†] and Zhiqiang Shi*[,‡]

[†]CAS Key Laboratory of Organic Solids, Beijing National Laboratory for Molecular Sciences (BNLMS), Institute of Chemistry, Chinese Academy of Sciences, Beijing, 100190, People's Republic of China

[‡]Shandong Normal University, 88 Wenhuadonglu Road, Jinan, 250014, People's Republic of China

Supporting Information

ABSTRACT: Large area (26.7 cm^2) nanotip arrays of porous conducting poly [5, 10, 15, 20-tetra (4-ethynylphenyl) porphyrin] diyne (TEPPD) have been successfully fabricated by an in situ cross-coupling reaction on the surface of the copper foil, which will open a new routine for large-area nanofabrication of porous conducting polymer on a conducting substrate. The surface-area of TEPPD nanotip arrays is up to 146 m^2/ g. Interestingly, the nanotip arrays of TEPPD display a good field-emission property and exhibit a better stability of field emission than that of organic and polymeric nanostructures because of the good heat radiation of porous, which is comparable to some important nanostructures of inorganic semiconductor. The porous conducting polymer could be used for new field-emission emitter and other molecular electronic devices.

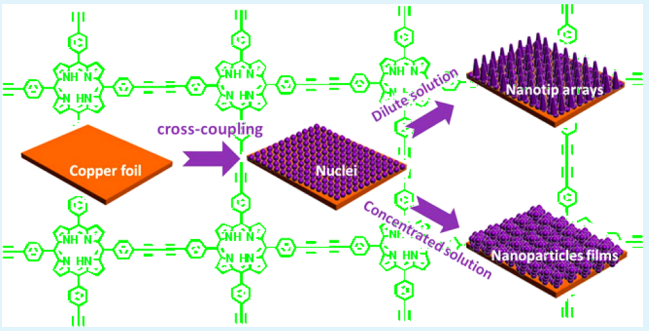

KEYWORDS: *porous conjugated polymer, nanotip arrays, large area, field emitter*

INTRODUCTION

In recent years, there has been immense interest in studying conjugated organic polymers due to their unique electrical and photoconduction properties.[1,2] In general, these conjugated polymers' optical, electronical, and opto-electronical properties can be significantly enhanced when they are confined to the nanoscale one-dimension.[3−7] Especially, vertically aligned free-standing nanowire/rod/nanotube arrays on conducting substrate would be ideal structures for electrical field emitters.[8−21] Some methods have been developed to produce conjugated polymer nanowire/rod arrays, for example, template,[22−29] polymer wetting or nanoimprint,[30−32] electropolymerization,[33,34] dilute polymerization,[35] polymerization followed by a recrystallization process,[36] and self-assembly combination method.[6,37−39] However, few conjugated polymers nanowire/rod arrays on large area (>cm^2) for field emitter can be prepared.[6] The field-emission stability of these conjugated polymers nanowire/rod arrays is not ideal because of their intrinsic low stability and poor heat radiation. Therefore, the development of growing scalable one-step technologies to produce pure and very large area (>cm^2) of conjugated polymer nanowire/rod arrays is very significant. Porous polymers have displayed various advantages in gas storage and separation, sensors and catalysts. Among of them, the porous conjugated polymers have attracted more attentions because they possess both functions of porous and conjugated polymers.[40−46] Specially, the porous structure of polymers is benefit to significantly improve electrical stability due to the good heat radiation of porous.

In view of the above-mentioned facts, we design 5,10,15,20-tetra (4-ethynylphenyl) porphyrin (TEPP) as a building block to fabricate large area (26.7 cm^2) porous conjugated polymer of poly[5,10,15,20-tetra (4-ethynylphenyl) porphyrin] diyne (TEPPD) nanotip arrays on the copper foil by in situ cross-coupling reaction. The surface-area of TEPPD nanotip with pore diameter of 2.7 nm is up to 146 m^2/ g. The nanotip arrays of TEPPD with 90 nm of top diameter displays good field emission property, the turn on field is 7.5 V/μm and threshold is 23.5 V/μm. Significantly, TEPPD nanotip arrays show the almost perfect stability on field emission because of its porous structure, which is better than that of polymeric nanostructures in previously, and is comparable to some important nanostructures of inorganic semiconductor. The porous conjugated polymers nanostructure will be a perspective potential field emitter. The results will expand the application of porous conjugated polymer and open a new door for designing new organic field-emission emitters.

EXPERIMENTAL SECTION

Synthesis of TEPPD nanotip arrays: 5,10,15,20-tetra (4-ethynylphenyl) porphyrin (TEPP) was synthesized via a three-step route as shown

Received: February 5, 2013
Accepted: March 12, 2013
Published: March 12, 2013

   dx.doi.org/10.1021/am4004914 | ACS Appl. Mater. Interfaces 2013, 5, 2761−2766

in Figure S1 in the Supporting Information according to the literature.[47] The TEPP was obtained as a purple powder in an overall yield of about 18% based on 4-Iodobenzaldehyde as the starting reagent. ^{1}HNMR (400 MHz, $CDCl_3$): 8.84(s, 8H), 8.18 (d, J = 8.0 Hz, 8H), 7.91(d, J = 8.0 Hz, 8H), 3.33(s, 4H), −2.83(s, 2H). MS: m/z = 711.3 M^+.

TEPP (5.3 mg, 0.0075 mmol) was dissolved with 25 mL of pyridine (dried with molecular sieve) in a three-mouth flask and added slowly over 12 h into 40 mL of pyridine including a copper foil with 6.2 × 4.3 cm^2 at reflux temperature under a nitrogen atmosphere. The copper foil was washed with 1 M HCl, deionized water and acetone, successively, and then blowed-dry with nitrogen gas in advance. The mixture was then refluxed for 2 days. A brown film was successfully grown on the surface of copper foil via a cross-coupling reaction (Figure 1). And then the copper foil covered with TEPPD film was rinsed by ethanol several times and blowed-dry with nitrogen gas to do further characterization.

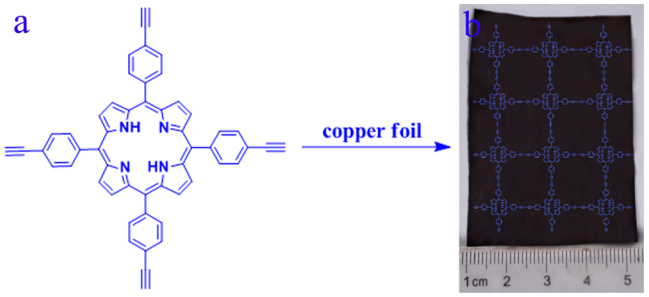

Figure 1. (a) Synthesis of TEPPD, (b) photograph of large-area TEPPD film on the Cu foil.

MATERIALS AND METHODS

All the reagents were purchased from Alfa Aesar Corp and Aldrich Corp, and all the solvents were purchased from Beijing Chemical reagent Corporation, China. Unless otherwise stated, all the reagents and solvents were used as received without further purification.

A copper foil (1 × 1 cm^2) covered with TEPPD film was characterized by the Attenuated Total Reflection Infrared Fourier transform infrared (ATR-IR) and Raman spectrum and the X-ray photoelectron spectrometer (XPS). The ATR-IR spectrograph was recorded on a Bruker EQUINOX55 ATR-IR spectrophotometer. Raman spectra were taken on a Renishaw-2000 Raman spectrometer at a resolution of 2 cm^{-1} by using the 533 nm line of an argon ion laser as the excitation source. The XPS was collected on a VGScientific ESCALab220i-XL X-ray photoelectron spectrometer using Al KR radiation as the excitation source. The banding energies obtained in the XPS analysis were corrected with reference to C 1s (284.8 eV). Field-emission scanning electron microscopy (FE-SEM) images and energy-dispersive X-microanalysis spectrum (EDS) were taken from Hitachi S-4800 FESEM microscope at an accelerating voltage of 5 kV and 15 kV using a copper foil (0.3 × 0.3 cm^2) covered with TEPPD film. Transmission electron microscopy (TEM) images and selective-area electron diffraction pattern (SAED) patterns were taken from JEOL JEM-2011 microscope at an accelerating voltage of 200 kV. For TEM measurement, 2 M HCl was used to corrode the copper foil covered with TEPPD film for 8 h, and the brown film was stripped. And then the film was washed by deionized water and dispersed in ethanol. The specific surface area was measured by ST-2000 BET surface area analyzer. The field emission properties of the TEPPD nanotip arrays were measured using a two-parallel-plate configuration in a homemade vacuum chamber at a base pressure of ~1 × 10^{-7} Torr at room temperature. The sample (be tested on the copper foil with 25 mm^2) is attached to one of the stainless-steel plates, which is the cathode, with the other plate acting as the anode. The distance between the electrodes was 200 μm, respectively. A direct current

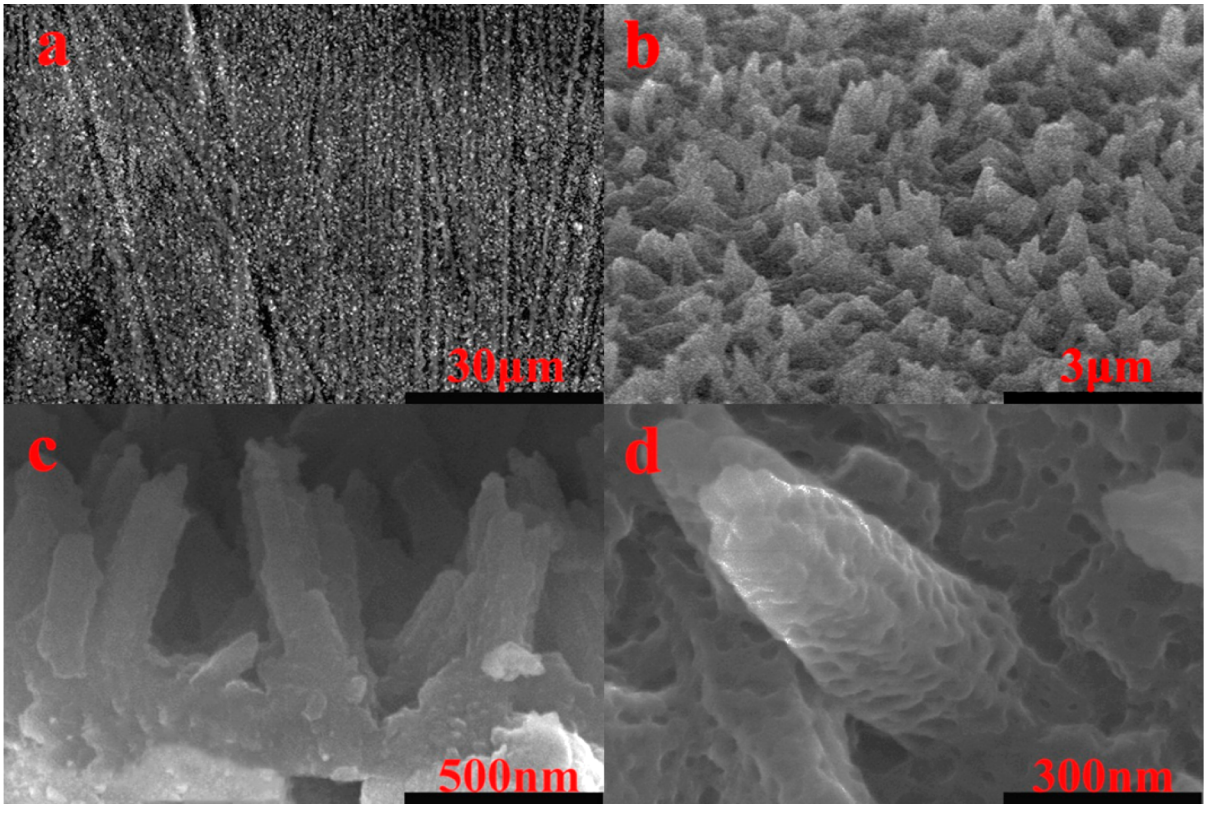

Figure 2. SEM images of the TEPPD nanotip arrays: (a) top view under low magnification, (b) side view under low magnification, (c) side view under higher magnification, (d) top view of a typical individual TEPPD nanotip.

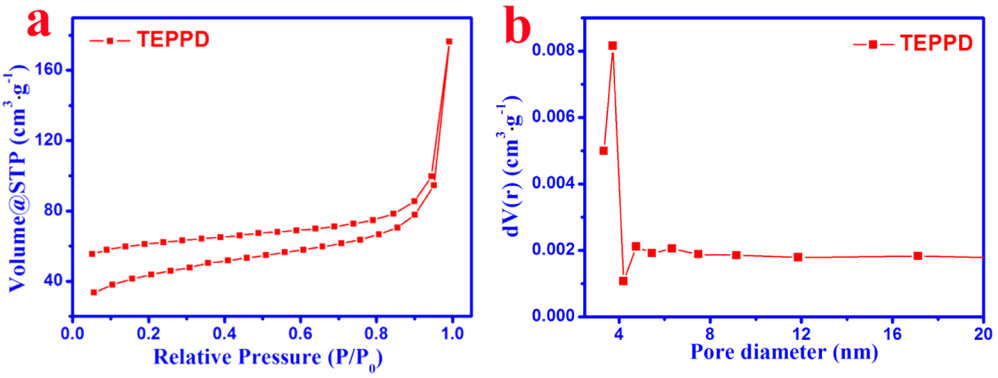

Figure 3. (a) BET examination of TEPPD nanotip arrays, (b) pore diameter examination of TEPPD nanotip arrays.

voltage sweeping from 0 to 7000 V was applied to the sample at a step of 50 V. The emission current was monitored using a Keithley 6485 picoammeter. The cyclic voltammograms was measured using a piece of TEPPD film with 1.3 × 2.5 cm^2 soaked in 0.1 mol/L n-Bu_4NPF_6 in acetonitrile.

RESULTS AND DISCUSSION

Figure 1b displays the photograph of as-prepared uniform blown film of TEPPD on Cu foil, whose area is up to 26.7 cm^2. The morphology of the TEPPD film is checked by SEM (Figure 2). As shown in Figure 2a–d, the TEPPD film is composed of continuous nanotip arrays. The diameter of uniform TEPPD nanotip is about 90 nm. The cross-sectional SEM image of TEPPD nanotip in Figure 2c shows that the TEPPD nanotips aligned on the surface of copper foil and its length is about 600 nm. Figure 2d is the SEM image of a typical individual TEPPD nanotip. The diameter of top and end of nanotip is 90 and 260 nm, respectively. Interestingly, the surface of TEPPD nanotip is porous. We can obtain more information of structure from TEM. Figure S2 in the Supporting Information shows TEM images of TEPPD nanotip, which confirm the tiplike structure of TEPPD. The length of TEPPD nanotip is about 600 nm. Under higher magnification of TEM (see Figure S2b in the Supporting Information), the diameter of the tip is about 90 nm, which agrees well with the SEM images. The SAED pattern shown in the inset of Figure S2b in the Supporting Information indicates the TEPPD nanotip is amorphous. HRTEM (see Figure S2c in the Supporting Information) demonstrated the porous structure of TEPPD nanotip, and the pore size is about 2.7 nm, which is consistent with the diameter of the intramolecular cavities of TEPPD. The result of EDS spectrum analysis (see Figure S3 in the Supporting Information) indicates that the TEPPD nanotip is composed of elemental carbon and nitrogen.

The as-prepared TEPPD nanotips film are confirmed by ATR-IR spectra (see Figure S4a in the Supporting Information), which provide evidence for the formation of TEPPD. Compared with the spectrum of monomer TEPP molecule, the spectrum of TEPPD nanotip arrays film shows obvious change. The typical C≡C stretching vibration band of 2188 cm^{-1} is observed, which is weak because of the molecular perfect symmetry.[48] The peaks at 1341 and 1597 cm^{-1} are typical absorption peaks of the benzene rings in porphyrin. The success of the preparing film of TEPPD nanotip arrays can be confirmed by the Raman spectrum of different position on the surface of copper foil (see Figure S4b in the Supporting Infomration). The peaks at 2206.0 cm^{-1} can be attributed to the vibration of conjugated diyne links (−C≡C−C≡C−).[48] The peaks at 1363.2 and 1560.3 cm^{-1} are contributed by the D band and the G band of the benzene rings in TEPPD, respectively. As shown in the fluorescence spectrum of Figure S4c in the Supporting Information, the emission of porphyrin at 654.8 and 719.7 nm obviously shift to longer wavelength 709.2 and 754.3 nm compared to the TEPP, respectively. The results indicate the formation of porphyrin polymer-TEPPD.[5,49] The results of BET demonstrate that the surface area is up to 146 m^2/g (Figure 3a), which confirms the porous structures of TEPPD, and the pore diameter is 3.1 nm, which agrees with the TEM images.

The as-prepared TEPPD nanotip arrays film is further confirmed by XPS spectra. The C 1s peak at 284.8 eV and N 1s peak at 398.6 eV in Figure S5a in the Supporting Information shows essentially identical binding energies for the C 1s and N 1s orbital, respectively. Figure S5b in the Supporting Information shows the narrow scan for element N, which can be deconvoluted into two subpeaks at 398.0 (C═N) and 399.3 eV (C−NH),[50] and the area ratio of them is 1:1, which agrees with the molecular structure of porphyrin. Figure S5c in the Supporting Information presents a high-resolution asymmetric C 1s XPS spectrum of the polymer, and the C 1s peak can be deconvoluted into mainly four subpeaks at 284.7, 285.2, 286.9, and 288.6 eV which have been assigned to the C 1s orbital of C−C (sp^2), C−C (sp), C−O, and C═O respectively.[51] The area ratio of sp/sp^2 is 2/11, which agrees with the ratio in TEPP. The Cu 2p peak at 935.8 eV is due to the existence of the copper foil, and the O 1s peak at 531.9 eV is contributed by the absorption of O_2. The results of XPS clearly demonstrate that the polymer is TEPPD. As shown in Figure S6 in the Supporting Information, the TEPPD nanotip arrays is stable under 350 °C and its weight reduce 17% at 430 °C, which indicates that TEPPD nanotip arrays has a high heat stability.

The mechanism of the formation of the TEPPD nanotip arrays is proposed as follows: The process of forming TEPPD is similar to the dilute polymerization (Scheme 1).[44,52,53] In this process, the copper foil is play the roles as not only catalyst for the cross-coupling reaction, but also as a substrate to provide the growing TEPPD nanotips film.[54,55] Trace amounts of Cu(II) ions can be formed to distribute on surface of the films in the presence of pyridine by the cross-coupling reaction.[44] The induction time is strongly dependent on the concentration of reagents in the polymerization. When very dilute monomer and Cu(II) as catalyst is used this reaction, heterogeneous nucleation was occurred first on the surface of solid substrates.[52,53] In our case, the concentration of Cu(II) ions and monomer TEPP are very dilute. In the beginning of

Scheme 1. Schematic Illustration of the Growth of TEPPD Nanotip Arrays on Copper Foil

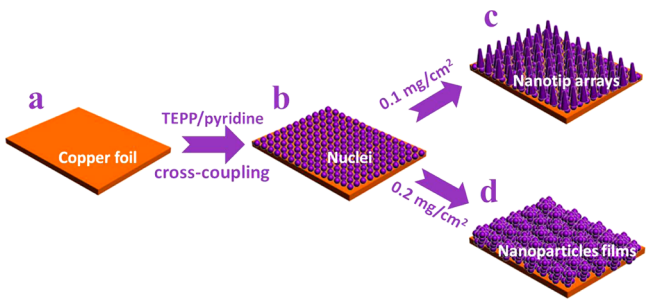

polymerization, the nucleation can be controlled to arise primarily on the surface of copper foil resulting in formation of many active nucleation centers (Scheme 1b), which minimize the interfacial energy barrier lead to subsequently the growth of TEPPD on the surface of copper foil. As well as TEPPD nanoparticles also can form as precipitation making some reactive oligomeric intermediates were consumed, resulting in the suppression of the growth rate of TEPPD on the copper foil. Thus, we can estimate the growth of TEPPD is only vertically from the active nucleation centers generated in the initial stage of polymerization. When the concentration of TEPP was 0.1 mg/cm^2, the TEPPD nanotip arrays can be obtained (Scheme 1c), and the concentration of TEPP was 0.2 mg/cm^2, the TEPPD nanoparticles films can be produced (Scheme 1d and Figure S7 in the Supporting Information).

As expected from the TEPPD nanotip arrays film, their excellent FE properties are observed. The FE measurements were performed out on the TEPPD nanotip arrays at a distance of 200 μm from the tips of the nanotip to the anode during the measurement. The current density-electric field (J–E) curves of the TEPPD nanotip arrays film and the TEPPD nanoparticles film are shown in Figure 4a. For all of the field emission analysis in this study, the turn-on field (E_{to}) and threshold field (E_{th}) are defined as the electronic fields required to produce a current density of 10 μA/cm^2 and 1 mA/cm^2, respectively. As shown in Figure 4a, the E_{to} of the TEPPD nanotip arrays and the TEPPD nanoparticles film is 7.5 and 16.1 V/μm, respectively. The E_{th} of the TEPPD nanotip arrays is 23.5 V/μm, and its maximum current density is up to 1.7 mA/cm^2, which is higher than that of most polymers and organic materials and comparable to some inorganic semiconductors.[56−64]

The field emission characteristics were further analyzed with the Fowler−Nordheim (F−N) theory. The Fowler−Nordheim curves (plotting $\ln(J/E^2)$ versus $1/E$) of the TEPPD nanotip arrays and the TEPPD nanoparticles film were shown in the inset of Figure 4a. The enhance factor β of field emission is in the direct ratio of the work function $\phi^{3/2}$ and in the inverse ratio of the slope (S) of the F−N plot:

$$S = -6.84 \times 103^3 \phi^{3/2}/\beta \quad (1)$$

where work function ϕ could be half of ionization potentials.[65]

$$\phi = \mathrm{IP}/2 \quad (2)$$

The onset potentials of the same electrolyte system can be used to determine the LUMO (E_{LUMO}) and HOMO (E_{HOMO}) energy levels,[66] and the difference between the two onset potentials should closely correspond to the band gap as well as the optical band gap.[67] The relationship of the energy levels, even ionization potentials (IP), and the electrochemical potentials can be expressed by eq 3.[66]

$$E_{HOMO} = \mathrm{IP} = -e(\Phi'_{ox} + 4.4) \quad (3)$$

where Φ'_{ox} is the onset of the first oxidation potential with all electrodes potential values vs SCE as the reference electrode. The onset potentials Φ'_{ox} (or Φ'_{red}) were determined from the intersection of the two tangents drawn at the rising oxidation (or reduction) current and background current in the cyclic voltammograms. As shown in Figure S8 in the Supporting Information, Φ'_{ox} of TEPPD is 0.4 eV, then the evaluated work function ϕ is about 2.4 eV. As shown in the inset of Figure 4a, the TEPPD nanotip arrays and the TEPPD nanoparticles film have a slope of F−N plot as about −39.5 and −231.0, and it can be calculated that the field-emission enhancement factor β of the TEPPD nanotip array film and the TEPPD nanoparticle film is 643.8 and 110.1, respectively, which indicates that TEPPD nanotip arrays have great potential as a competitive candidate for field emitters.

To evaluate the field-emission stability of the TEPPD nanotip arrays film, the current density over 3000 s with starting current densities of 1 mA/cm^2 was monitored, as shown in Figure 4b. The observations of the TEPPD nanotip arrays film show that no obvious degradation of current density was detected during a period of 3000 s of continuous emission, which demonstrates that TEPPD nanotip arrays have a high stability of field emission. The excellent field-emission stability

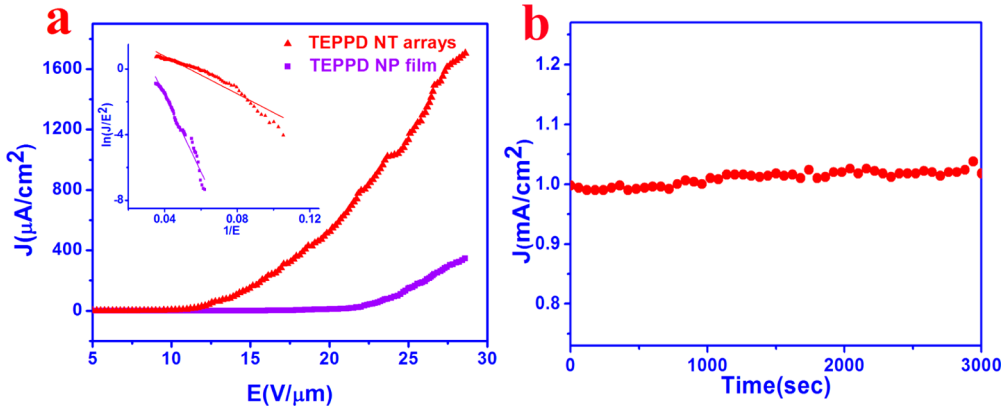

Figure 4. (a) Field-emission J–E curves of the TEPPD nanotip arrays and the TEPPD nanoparticles film. The inset is field-emission Fowler–Nordheim curves. (b) Field-emission stability of the TEPPD nanotip arrays.

dx.doi.org/10.1021/am4004914 | ACS Appl. Mater. Interfaces 2013, 5, 2761−2766

is mainly due to the chemically and physically stable structures of TEPPD nanotip arrays. Another key factor of the high field-emission stability is the porous structure of TEPPD nanotips, which is conducive to the heat radiation on the process of field emission.

CONCLUSIONS

In summary, we have demonstrated an in situ cross-coupling reaction to first generate large area (26.7 cm^2) nanotip arrays of new porous conjugated polymer TEPPD on the surface of the copper foil. The surface-area of nanotip arrays of TEPPD with pore diameter of 2.7 nm is up to 146 m^2/ g. Because of the good heat radiation of porous structure, the nanotip arrays of TEPPD exhibit almost perfect stability on field emission, which is comparable to most of inorganic semiconductor nanostructures and better than that of organic nanostructures. We think that the nanotip arrays of porous conjugated polymers might have applicability for fundamental research in the field of nanoscience and nanotechnology, with great potential to produce new field-emission emitter and other molecular electronic devices. The above results will expand the application of porous conjugated polymer and open a new door for designing new organic field-emission emitters.

ASSOCIATED CONTENT

Supporting Information

Synthesis and molecular structure of TEPP, TEM images of TEPPD nanotip arrays, IR, Raman, fluorescence and XPS spectra of the TEPPD nanotip arrays, thermo gravimetric analysis curve of the TEPPD nanotip arrays, SEM images of the TEPPD nanoparticles film and cyclic voltammograms of TEPPD. This material is available free of charge via the Internet at http://pubs.acs.org.

AUTHOR INFORMATION

Corresponding Author

*E-mail: liuhb@iccas.ac.cn (H.L.); zshi@sdnu.edu.cn (Z.S.).

Notes

The authors declare no competing financial interest.

ACKNOWLEDGMENTS

This work was supported by the National Basic Research 973 Program of China (2011CB932302 and 2012CD932900) and the National Nature Science Foundation of China (21031006 and 90922007).

REFERENCES

(1) Tran, H. D.; Li, D.; Kaner, R. B. *Adv. Mater.* **2009**, *21*, 1487.
(2) Zhou, W. D.; Li, Y. L.; Zhu, D. B. *Chem—Asian J.* **2007**, *2*, 222.
(3) Kim, K.; Shin, J. W.; Lee, Y. B.; Cho, M. Y.; Lee, S. H.; Park, D. H.; Jang, D. K.; Lee, C. J.; Joo, J. *ACS Nano* **2010**, *4*, 4197.
(4) Shirakawa, M.; Fujita, N.; Shinkai, S. *J. Am. Chem. Soc.* **2005**, *127*, 4164.
(5) Duncan, T. V.; Susumu, K.; Sinks, L. E.; Therien, M. J. *J. Am. Chem. Soc.* **2006**, *128*, 9000.
(6) Gan, H. Y.; Liu, H. B.; Li, Y. J.; Zhao, Q.; Li, Y. L.; Wang, S.; Jiu, T. G.; Wang, N.; He, X. R.; Yu, D. P.; Zhu, D. B. *J. Am. Chem. Soc.* **2005**, *127*, 12452.
(7) Xiao, J. C.; Kusuma, D. Y.; Wu, Y. C.; Boey, F.; Zhang, H.; Lee, P. S.; Zhang, Q. C. *Chem-Asian J.* **2011**, *6*, 801.
(8) Sonmez, G.; Meng, H.; Zhang, Q. C.; Wudl, F. *Adv. Funct. Mater.* **2003**, *13*, 726.
(9) Wang, Z. L.; Song, J. H. *Science* **2006**, *312*, 242.
(10) Lee, C.-Y.; Lu, M.-P.; Liao, K.-F.; Wu, W.-W.; Chen, L.-J. *Appl. Phys. Lett.* **2008**, 93.
(11) Cho, S. I.; Lee, S. B. *Acc. Chem. Res.* **2008**, *41*, 699.
(12) Wang, K.; Huang, J. Y.; Wei, Z. X. *J. Phys. Chem. C* **2010**, *114*, 8062.
(13) Musa, I.; Munindrasdasa, D. A. I.; Amaratunga, G. A. J.; Eccleston, W. *Nature* **1998**, *395*, 362.
(14) Wang, C. W.; Wang, Z.; Li, M. K.; Li, H. L. *Chem. Phys. Lett.* **2001**, *341*, 431.
(15) Kim, B. H.; Kim, M. S.; Park, K. T.; Lee, J. K.; Park, D. H.; Joo, J.; Yu, S. G.; Lee, S. H. *Appl. Phys. Lett.* **2003**, *83*, 539.
(16) Joo, J.; Kim, B. H.; Park, D. H.; Kim, H. S.; Seo, D. S.; Shim, J. H.; Lee, S. J.; Ryu, K. S.; Kim, K.; Jin, J. -I.; Lee, T. J.; Lee, C. J. *Synth. Met.* **2005**, *153*, 313.
(17) Joo, J.; Park, S.-K.; Seo, D.-S.; Lee, S.-J.; Kim, H.-S.; Ryu, K.-S.; Lee, T.-J.; Seo, S.-H.; Lee, C.-J. *Adv. Funct. Mater.* **2005**, *15*, 1465.
(18) Peng, J. B.; Huang, W. B.; Zhu, Z. S. *Synth. Met.* **2003**, *135*, 193.
(19) Yan, H. L.; Zhang, L.; Shen, J. Y.; Chen, Z. J.; Shi, G. Q.; Zhang, B. L. *Nanotechnol.* **2006**, *17*, 3446.
(20) Kim, J.; Choi, J.; Son, Y.; Lee, Y.; Yang, J.-H.; Park, C.-Y.; Park, J.-H.; Yoo, J.-B. *Mol. Cryst. Liq. Cryst.* **2007**, *462*, 117.
(21) Suen, S.-C.; Whang, W.-T.; Hou, F.-J.; Dai, B.-T. *Org. Electron.* **2006**, *7*, 428.
(22) Liu, H. B.; Li, Y. L.; Jiang, L.; Luo, H. Y.; Xiao, S. Q.; Fang, H. J.; Li, H. M.; Zhu, D. B.; Yu, D. P.; Xu, J.; Xiang, B. *J. Am. Chem. Soc.* **2002**, *124*, 13370.
(23) Guo, Y. B.; Tang, Q. X.; Liu, H. B.; Zhang, Y. J.; Li, Y. L.; Hu, W. P.; Wang, S.; Zhu, D. B. *J. Am. Chem. Soc.* **2008**, *130*, 9198.
(24) Cao, Y.; Mallouk, T. E. *Chem. Mater.* **2008**, *20*, 5260.
(25) Martin, C. R. *Science* **1994**, *266*, 1961.
(26) Zhang, X.; Manohar, S. K. *J. Am. Chem. Soc.* **2005**, *127*, 14156.
(27) Niu, Z.; Bruckman, M.; Kotakadi, V. S.; He, J.; Emrick, T.; Russell, T. P.; Yang, L.; Wang, Q. *Chem. Commun.* **2006**, 3019.
(28) Steinhart, M.; Wendorff, J. H.; Greiner, A.; Wehrspohn, R. B.; Nielsch, K.; Schilling, J.; Choi, J.; Gosele, U. *Science* **2002**, *296*, 1997.
(29) Chen, N.; Qian, X. M.; Lin, H. W.; Liu, H. B.; Li, Y. L. *J. Mater. Chem.* **2012**, *22*, 11068.
(30) Steinhart, M.; Wehrspohn, R. B.; Gösele, U.; Wendorff, J. H. *Angew. Chem., Int. Ed.* **2004**, *43*, 1334.
(31) Shin, K.; Xiang, H. Q.; Moon, S. I.; Kim, T.; McCarthy, T. J.; Russell, T. P. *Science* **2004**, *306*, 76.
(32) García-Gutiérrez, M.-C.; Linares, A.; Hernández, J. J.; Rueda, D. R.; Ezquerra, T. A.; Poza, P.; Davies, R. J. *Nano Lett.* **2010**, *10*, 1472.
(33) Lee, J. I.; Cho, S. H.; Park, S.-M.; Kim, J. K.; Kim, J. K.; Yu, J.-W.; Kim, Y. C.; Russell, T. P. *Nano Lett.* **2008**, *8*, 2315.
(34) Kim, J. K.; Yang, S. Y.; Lee, Y.; Kim, Y. *Prog. Polym. Sci.* **2010**, *35*, 1325.
(35) Chiou, N.-R.; Lu, C.; Guan, J.; Lee, L. J.; Epstein, A. J. *Nat. Nanotechnol.* **2007**, *2*, 354.
(36) Tang, Q. W.; Wu, J. H.; Sun, X. M.; Li, Q. H.; Lin, J. M. *Langmuir* **2009**, *25*, 5253.
(37) Kuila, B. K.; Nandan, B.; Bohme, M.; Janke, A.; Stamm, M. *Chem. Commun.* **2009**, 5749.
(38) Wang, Y.; Tran, H. D.; Kaner, R. B. *J. Phys. Chem. C* **2009**, *113*, 10346.
(39) Ryu, J.; Park, C. B. *Adv. Mater.* **2008**, *20*, 3754.
(40) Chen, Q.; Luo, M.; Hammershøj, P.; Zhou, D.; Han, Y.; Laursen, B. W.; Yan, C.-G.; Han, B.-H. *J. Am. Chem. Soc.* **2012**, *134*, 6084.
(41) Weber, J.; Thomas, A. *J. Am. Chem. Soc.* **2008**, *130*, 6334.
(42) Jiang, J.-X.; Su, F.; Trewin, A.; Wood, C. D.; Campbell, N. L.; Niu, H.; Dickinson, C.; Ganin, A. Y.; Rosseinsky, M. J.; Khimyak, Y. Z.; Cooper, A. I. *Angew. Chem., Int. Ed.* **2007**, *46*, 8574.
(43) Jiang, J.-X.; Su, F.; Trewin, A.; Wood, C. D.; Niu, H.; Jones, J. T. A.; Khimyak, Y. Z.; Cooper, A. I. *J. Am. Chem. Soc.* **2008**, *130*, 7710.
(44) Yuan, S. W.; Dorney, B.; White, D.; Kirklin, S.; Zapol, P.; Yu, L. P.; Liu, D.-J. *Chem. Commun.* **2010**, *46*, 4547.
(45) Shultz, A. M.; Farha, O. K.; Hupp, J. T.; Nguyen, S. T. *Chem. Sci.* **2011**, *2*, 686.

(46) Schmidt, J.; Weber, J.; Epping, J. D.; Antonietti, M.; Thomas. *Adv. Mater.* **2009**, *21*, 702.
(47) Chan, C.-S.; Tse, A. K. S.; Chan, K. S. *J. Org. Chem.* **1994**, *59*, 6084.
(48) Haley, M. M. *Pure Appl. Chem.* **2008**, *80*, 519.
(49) Huang, C. S.; Wang, N.; Li, Y. L.; Li, C. H.; Li, J. B.; Liu, H. B.; Zhu, D. B. *Macromolecules* **2006**, *39*, 5319.
(50) Sarno, D. M.; Matienzo, L. J.; Jones, W. E. *Inorg. Chem.* **2001**, *40*, 6308−6315.
(51) Estrade-Szwarckopf, H. *Carbon* **2004**, *42*, 1713.
(52) Liang, L.; Liu, J.; Windisch, J. C. F.; Exarhos, G. J.; Lin, Y. *Angew. Chem., Int. Ed.* **2002**, *41*, 3665.
(53) Liu, J.; Lin, Y. H.; Liang, L.; Voigt, J. A.; Huber, D. L.; Tian, Z. R.; Coker, E.; McKenzie, B.; McDermott, M. J. *Chem.—Eur. J.* **2003**, *9*, 605.
(54) Li, G. X.; Li, Y. L.; Liu, H. B.; Guo, Y. B.; Li, Y. J.; Zhu, D. B. *Chem. Commun.* **2010**, *46*, 3256.
(55) Hebert, N.; Beck, A.; Lennox, R. B.; Just, G. *J. Org. Chem.* **1992**, *57*, 1777.
(56) Wang, Z. Q.; Day, P. N.; Pachter, R. *J. Chem. Phys.* **1998**, *108*, 2504.
(57) Wu, Y. H.; Yang, B. J.; Zong, B. Y.; Sun, H.; Shen, Z. X.; Feng, Y. P. *J. Mater. Chem.* **2004**, *14*, 469.
(58) Qian, X. M.; Liu, H. B.; Guo, Y. B.; Song, Y. L.; Li, Y. L. *Nanoscale Res. Lett.* **2008**, *3*, 303.
(59) Qian, X. M.; Liu, H. B.; Guo, Y. B.; Zhu, S. Q.; Song, Y. L.; Li, Y. L. *Nanoscale Res. Lett.* **2009**, *4*, 955.
(60) Liu, H. B.; Zhao, Q.; Li, Y. L.; Liu, Y.; Lu, F. S.; Zhuang, J. P.; Wang, S.; Jiang, L.; Zhu, D. B.; Yu, D. P.; Chi, L. F. *J. Am. Chem. Soc.* **2005**, *127*, 1120.
(61) Cui, S.; Liu, H. B.; Gan, L. B.; Li, Y. L.; Zhu, D. B. *Adv. Mater.* **2008**, *20*, 2918.
(62) Liu, H. B.; Xu, J. L.; Li, Y. J.; Li, Y. L. *Acc. Chem. Res.* **2010**, *43*, 1496.
(63) Cui, S.; Li, Y. L.; Guo, Y. B.; Liu, H. B.; Song, Y. L.; Xu, J. L.; Lv, J.; Zhu, M.; Zhu, D. B. *Adv. Mater.* **2008**, *20*, 309.
(64) Zheng, H. Y.; Li, Y. J.; Liu, H. B.; Yin, X. D.; Li, Y. L. *Chem. Soc. Rev.* **2011**, *40*, 4506.
(65) Ashcroft, N. W.; Mermin, N. D. *Solid State Physics*; Thomson Learning: Stamford, CT, 1976; p 354
(66) deLeeuw, D. M.; Simenon, M. M. J.; Brown, A. R.; Einerhand, R. E. F. *Synth. Met.* **1997**, *87*, 53.
(67) Eckhardt, H.; Shacklette, L. W.; Jen, K. Y.; Elsenbaumer, R. L. *J. Chem. Phys.* **1989**, *91*, 1303.